Environmental Science
Water Research & Technology

ROYAL SOCIETY OF CHEMISTRY

PAPER

View Article Online
View Journal | View Issue

Cite this: *Environ. Sci.: Water Res. Technol.*, 2023, **9**, 1672

Evaluation of membrane fouling in a microalgal-bacterial membrane photobioreactor treating secondary wastewater effluent: effect of photoperiod conditions

E. Segredo-Morales, [a] E. González, *[a] C. González-Martín[b] and L. Vera [a]

Received 28th February 2023,
Accepted 19th April 2023

DOI: 10.1039/d3ew00138e

rsc.li/es-water

Microalgal-bacterial membrane photobioreactors (MPBRs) have emerged as a transformative wastewater treatment technology for reducing carbon emissions whilst achieving high quality effluent. However, membrane fouling negatively affects process performance by increasing energy consumption and reducing membrane lifespan. In this study, light/dark photoperiods were varied to optimize treatment performance and biomass properties and reduce membrane fouling. Increasing the length of the light period favored higher production of biomass but decreased bioflocculation. An intermediate photoperiod of 16/8 h achieved high values of biomass concentration (3.21 ± 0.45 g L^{-1}) and nutrient removal rates (4.71 mg N L^{-1} d^{-1} and 0.67 mg P L^{-1} d^{-1}, respectively), while preventing accumulation of biopolymer clusters (≤5.5 mg DOC L^{-1}) in the suspension. In addition, short-term fouling—associated with floc deposition forming a cake layer—was minimized at intermediate photoperiods, thus increasing the sustainable (*i.e.*, threshold) permeate flux. Under these sustainable flux conditions, membrane fouling was mainly determined by the biopolymer cluster content, with best performance being attained at 16/8 h. The above results reveal that the photoperiod is a crucial parameter for controlling membrane fouling in microalgal-bacterial membrane photobioreactors.

Water impact

The microalgal-bacterial membrane photobioreactor is a promising approach for sustainable wastewater reclamation. However, its widespread application is limited by the high costs associated with membrane fouling. Due to complex interactions among indigenous consortia, selecting optimal conditions is challenging. This study demonstrated that long-term fouling is minimized at intermediate light/dark photoperiods, which also allows high biomass concentration and effective nutrient removal.

1. Introduction

Progressive decarbonization is prompting the wastewater treatment sector to search for transformative technologies that can increase energy efficiency, recover resources and prevent greenhouse gases emissions.[1,2] Recently, novel treatment technologies, such as photocatalysis,[3] microwave catalysis[4,5] or zero-valent iron nanoparticles[6] have been proposed. Nevertheless, although these are promising technologies, there are several disadvantages that have to be addressed to ensure their safe and effective use in wastewater treatment. Further investigation on catalysis deactivation, safety hazards due to microwave radiation or release of nanoparticles into the environment, is needed before practical use. Alternatively, a photobioreactor system based on microalgae-bacteria consortia is a promising approach to achieve sustainable wastewater technologies.[7–9] In a symbiotic relationship, microalgae produce dissolved oxygen, which can be used for bacterial respiration (oxidizing organic matter, ammonium and nitrite), reducing operating costs resulting from mechanical aeration. In turn, the carbon dioxide generated is used by the microalgae for carbon anabolism. Additionally, microalgae-bacteria consortia recover nutrients from wastewater through biomass synthesis. Produced biomass can be further valorized into added-value products, such as biogas or agricultural products.[10,11] Likewise, the move to a circular economy needs to be accomplished through the consistent promotion of safe

[a] *Departamento de Ingeniería Química y Tecnología Farmacéutica, Universidad de La Laguna, Astrofísico, Fco, Sánchez s/n, 38200 La Laguna, Spain. E-mail: esegredm@ull.edu.es, eglezc@ull.es, luvera@ull.edu.es*
[b] *Instituto Universitario de Enfermedades Tropicales y Salud Pública de Canarias, Universidad de La Laguna, Astrofísico, Fco, Sánchez s/n, 38200 La Laguna, Spain. E-mail: cgonzama@ull.edu.es*

water re-use.[12] Current advanced systems combine biological treatment with microfiltration or ultrafiltration membranes to produce high-quality effluents that are suitable for most industrial applications, including highly demanding agriculture irrigation.[13,14]

A technology now actively being investigated is a microalgal-bacterial membrane photobioreactor (MPBR), which combines suspended biomass with immersed microfiltration or ultrafiltration membranes.[15,16] This technology has demonstrated the capability to efficiently treat municipal wastewaters[17] or secondary effluents.[18,19] Hydraulic and solid retention times (HRT and SRT, respectively) are commonly studied parameters, mainly focused on nutrient removal and biomass productivity.[15,20] Another important factor affecting microalgal-bacterial processes is light availability, mainly determined by light intensity and photoperiods.[21,22] Typically, microalgae activity increases with light intensity up to a saturation point (~200–540 μmol m^{-2} s^{-1}), which is species dependent, above which the effect becomes insignificant.[23] Indeed, in many species, increasing intensity results in photoinhibition thus reducing microalgae growth rate.[24] A similar behavior has been reported for nitrifying bacteria, particularly nitrite oxidizers, which show significant photoinhibition above 500 μmol m^{-2} s^{-1}.[25] Nevertheless, several strategies can be applied to control light intensity by modifying reactor design (*i.e.* culture depth) or biomass concentration (affecting light shading effect).[8] Regarding the photoperiod, microalgae growth rate is generally enhanced by extending the light period from 12/12 to 24/0 h (continuous illumination),[26,27] but several studies have reported no appreciable effect[28] or even a decrease in the growth rate.[29] These contradictory findings suggest that photoperiod, light intensity and light shading may be interrelated.

A critical constraint of MBPR technology development at an industrial scale is the inherent membrane fouling.[30,31] In general, the extent of fouling is a complex function of biomass characteristics, operating conditions and membrane properties.[20] To alleviate membrane fouling, common practices in MPBRs are the use of moderate permeate fluxes, membrane air scouring, physical cleaning methods (relaxation and backwashing) and chemical cleanings.[19,32] Fouling can be classified into two main categories based on membrane permeability recovery by physical methods. The first is reversible fouling, which can be removed by physical means and is mainly attributed to cake layer development and possibly to pore blocking. The second category is residual fouling (also called physically irreversible fouling), which mainly refers to adsorption of foulants and gel formation, and is only removed by chemical means.[33] These phenomena lead to a loss in membrane permeability, higher energy consumption and more frequent chemical cleanings, which can reduce the membrane's lifespan.[34] Most previous studies assessing membrane fouling in MPBR have focused on biomass characteristics, particularly biomass concentration, particle size distribution and supernatant biopolymers content.[30,35–39] Main influencing factors assessed in these studies are hydraulic and solid retention times, feedwater characteristics (nitrogen source and ratio of N/P) and alga/activated sludge inoculation ratios. Nevertheless, although light is a key parameter in microalgae-bacteria consortia growth and biomass properties, it has been less studied. In fact, a previous study revealed a trade-off between biomass productivity/nutrient removal and membrane fouling.[40] In this work it is reported that reducing the light path in a photobioreactor (*i.e.* increasing photosynthetic efficiency) significantly increases the membrane fouling rate. Therefore, finding optimal illumination conditions (intensity and/or photoperiod) would considerably improve operational feasibility and reduce the cost of MPBR technology.

This study focuses on assessing the effect of the photoperiod on the performance of a MPBR, particularly on membrane fouling. The assessment was conducted by analyzing treatment performance and main biomass properties, such as concentration, elemental composition, particle size distribution and supernatant biopolymers content. Using a flux-step method, fouling propensity and sustainable flux conditions were investigated. Finally, long-term fouling tests verified sustainable membrane performance by assessing residual fouling evolution.

2. Materials and methods.

2.1. Feedwater

The MPBR unit was fed with a secondary effluent obtained from a conventional activated sludge wastewater treatment plant (Santa Cruz de Tenerife, Canary Island, Spain), which was designed for organic matter removal. Main physical–chemical characteristics are given in Table 1.

2.2. MPBR set-up

The experimental unit consisted of a cylindrical 3.0 L (diameter = 14 cm) MPBR equipped with ZeeWeed® ZW-1 (Suez Water Technologies & Solutions, Ontario, ON, Canada) hollow fiber membranes with a nominal pore size of 0.04 μm and 1.9 mm outer diameter, assembled vertically, which provide 0.047 m^2 of filtering surface area (Fig. 1). ZeeWeed® consists of a woven reinforcing braid on which a PVDF

Table 1 Main physical–chemical characteristics of the feedwater (n = 55)

Parameters	Units	Mean	Range
COD	mg L^{-1}	67.2	39–113
DOC	mg L^{-1}	17.9	12.7–45.7
pH	—	8.2	7.9–8.4
$N–NH_4^+$	mg L^{-1}	25.8	2.5–41.9
$N–NO_3^-$	mg L^{-1}	2.0	0–12.9
$N–NO_2^-$	mg L^{-1}	1.7	0–9.5
$P–PO_4^{3-}$	mg L^{-1}	4.1	0.8–7.9
CO_3^{2-}	mg L^{-1}	8.5	0–21.6
HCO_3^-	mg L^{-1}	552.6	414.0–698.7
Turbidity	NTU	2.0	1.1–5.0
TSS	mg L^{-1}	4.5	0–22

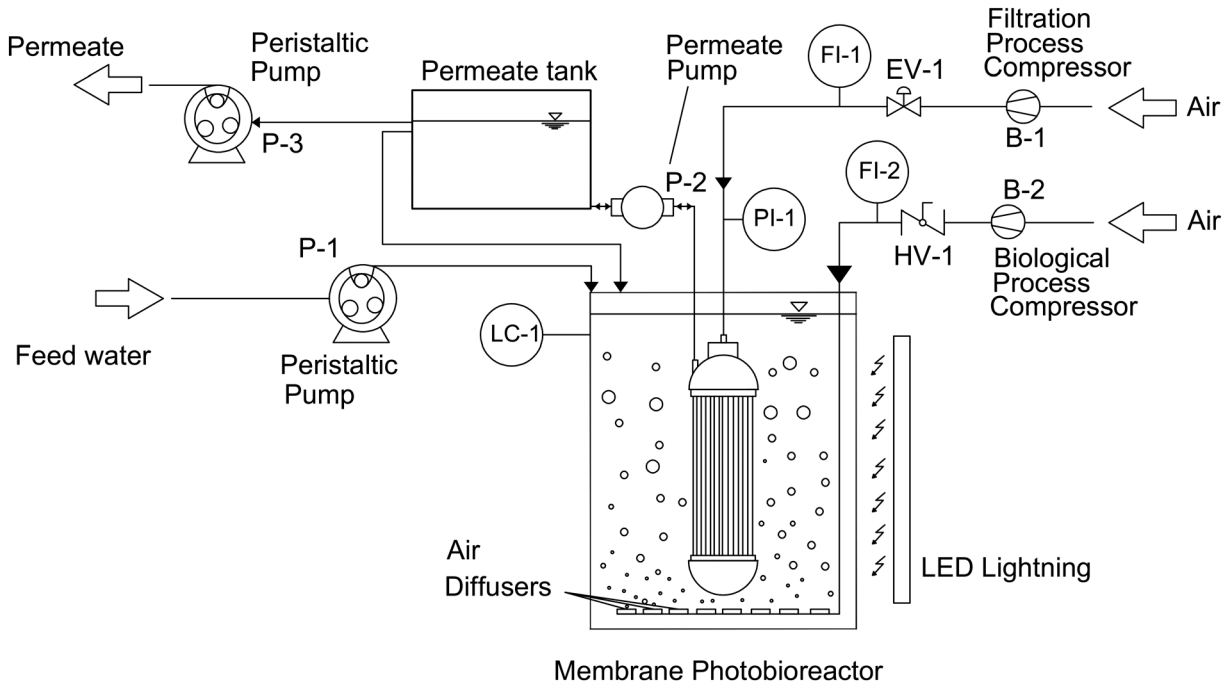

Fig. 1 Schematic diagram of the MPBR system.

membrane is cast. The permeate was extracted by a magnetic drive gear pump (Micropump-GA Series, Stockholm, Sweden) applying a slight vacuum. All the experiments were conducted at a permeate flux (J) of 10 L h^{-1} m^{-2}, measuring transmembrane pressure (TMP) with a pressure sensor (Sensotec, Barcelona, Spain). To prevent severe membrane fouling, the system operated under consecutive filtration/backwashing cycles of 450/30 s combined with intermittent air scouring (10/30 s on/off) at 5 NL min^{-1} during the filtration. The backwash flux was set at 30 L h^{-1} m^{-2} with continuous aeration at 5 NL min^{-1}. DAQ Factory software (AzeoTech® Inc., Ashland, OR, USA) was used for visualization and control of the filtration variables.

Air was also injected at the bottom of the MPBR at 1 NL min^{-1} to provide aerobic conditions and mix the biological suspension. Dissolved oxygen concentration and pH were within the ranges of 6.9–9.6 mg L^{-1} and 8.1–8.9, respectively, throughout all experiments. The system was run at HRT and SRT values of 0.75 d and 80 d, respectively. The former was within the typical range of operating values in MPBRs[41] and the latter was selected according to a previous study on enhancing bioflocculation and avoiding biopolymer cluster accumulation.[42] The effluent was extracted from the permeate tank by a peristaltic pump (Cole-Parmer Instrument Co., USA) according to the selected HRT. To maintain a constant HRT regardless of permeate flux, excess permeate was returned to the MPBR. Experiments were carried out at room temperature (19 ± 1 °C) under constant irradiation of 300 μmol m^{-2} s^{-1} measured at the surface of the photobioreactor (PAR irradiance using an irradiance meter, QSP2150A, Biospherical Instruments Inc., USA). The aim of the experiments was to assess the impact of photoperiods on the MPBR performance. To do this, four long-term experiments of 900 h were carried out under different light/dark photoperiods (0/24, 12/12, 16/8 and 24/0 h).

Before starting each experiment, the system was initially filled only with feedwater. Then, it was operated at 0.75 d of HRT for a minimum of 80 d without biomass purge. Thus, the system started without inoculum and the biomass developed from indigenous microorganisms. After the acclimation period, the biomass was manually purged to maintain the desired SRT. This procedure allowed the biomass concentration to remain stable during the experiments.

Samples of feedwater, suspension and permeate were analyzed three times per week. Suspensions were characterized by particles size, mixed liquor suspended solids (MLSS), volatile matter, elemental composition (C, N and H), supernatant dissolved organic carbon (DOC) and suspended solids (SS), and Fourier-transform infrared spectroscopy (FTIR). The average biomass productivity (r_x) was estimated following eqn (1):

$$r_x = \frac{\mathrm{MLSS}}{\mathrm{SRT}} \quad (1)$$

2.3. Short-term flux step trials

A flux-step method with intermediate backwashing cycles was applied.[43] Main parameters were: flux range of 8–40 L h^{-1} m^{-2}, flux increment of 2 L h^{-1} m^{-2} and step duration of 15 min. Air scouring and backwashing conditions were the same as those applied in the long-term experiments. The flux-step trials were carried out with the suspensions and supernatants (obtained after 30 min of decantation and transferred into a clean vessel). Before each run, the membrane was chemically

cleaned using a 500 mg L^{-1} of NaClO for 24 h. Reversible fouling was assessed by the fouling rate (r_f), given by the change in transmembrane pressure with time (dTMP/dt).

2.4. Membrane cleaning protocol

After the long-term fouling tests, the fouled membrane was subjected to a cleaning protocol that included the following steps:[44] (1) rinsing with tap water, (2) chemical cleaning with NaClO (500 mg L^{-1}) for 24 h, and (3) chemical cleaning with citric acid (6 g L^{-1}) for 2 h. After each step, the hydraulic resistance was calculated using a tap water filtration test.

2.5. Membrane fouling characterization

During the long-term tests, TMP evolution with consecutive filtration/backwashing was used to assess membrane fouling. It can be described by the following equation:[43]

$$TMP = TMP_i + r_f \cdot t \quad (2)$$

where TMP_i is the initial transmembrane pressure at the beginning of each filtration cycle, r_f is the reversible fouling rate and t is the elapsed time.

Eqn (2) assumes a constant r_f during the filtration phases, describing an incompressible cake development mechanism on the membrane wall. On the other hand, TMP_i is related to residual fouling, which cannot be removed by physical means. Both parameters have been widely used to describe membrane fouling in conventional membrane bioreactors (MBRs).[33]

2.6. Analytical methods

Dissolved oxygen was measured using an oximeter Hach Lange LDO (USA). Total suspended solids (TSS), mixed liquor suspended solids (MLSS) and chemical oxygen demand (COD) were analyzed according to the standard methods.[45] Nitrogen–ammonium ($N–NH_4^+$) was analyzed by the Nessler method using a DR-5000 Hach spectrophotometer (USA). Nitrogen–nitrite ($N–NO_2^-$), nitrogen–nitrate ($N–NO_3^-$) and phosphorus–phosphate ($P–PO_4^{3-}$) were analyzed by ion chromatography using a Compact IC plus 882 device, supplied by Metrohm. Total dissolved inorganic nitrogen (DIN) was obtained by adding $N–NH_4^+$, $N–NO_2^-$ and $N–NO_3^-$. Dissolved organic carbon (DOC) concentration was measured with a TOC-meter (TOC-5000A, Shimadzu, Japan). The DOC difference between the filtered supernatant (through a filter of glass-fiber with a nominal pore size of 1.2 μm) and the permeate was assigned as biopolymers clusters (BPC) concentration. Particle size distribution was analyzed using Malvern Mastersizer 2000 (UK) laser diffraction particle size analyzer with a detection range of 0.02–2000 μm. FLASH EA 1112 Elemental Analyzer (ThermoFisher Scientific, USA) was used for the elemental analysis. Samples were previously dried in an oven at 100 °C for 1 h. Volatile matter was measured by a thermal analyzer (TG/DSC): Discovery SDT 650 (TA Instruments, USA). Fourier-transform infrared spectrometry was performed using an IFS 66/S spectrometer (Bruker, USA) equipped with an ATR accessory that measured the transmittance of the samples in a wavelength range between 900 and 4000 cm^{-1}. Microalgae identification was conducted by optical microscopy (DM750, Leica, Germany) according to Wastewater Organisms Atlas Manual.[46] Detection of *Escherichia coli* and *Legionella* spp. was performed in the permeate according to ISO 9308 and ISO 11731, respectively, as recommended by the legislation.

2.7. Statistical analysis

The results were analyzed by OriginPro (OriginLab Corporation, MA, USA). Analysis of variance (one-way ANOVA) and Tukey's test was used to assess differences between photoperiods. Significance was assumed when p-values <0.05.

3. Results and discussion.

3.1. Biomass productivity and characteristics

As shown in Fig. 2a, longer lighting periods significantly influenced biomass concentration and productivity. Maximum biomass concentration (3.21 ± 0.45 g L^{-1}) was obtained at 16/8 h photoperiod (light/dark), which did not increase at continuous illumination ($p > 0.05$). Compared to operation at 0/24 h (control condition), the results revealed a significant growth of microalgae in the mixed consortia (representing approximately a 30-fold increase), which achieved a productivity value of 40.1 mg L^{-1} d^{-1}. Indeed, microalgae belonging to the genera *Scenedesmus* and *Chorella* were identified in abundance. This is consistent with those productivities usually reported for MBPRs operated at long SRTs with secondary effluents (28–41 mg L^{-1} d^{-1}).[22] Nevertheless, the fact that productivity did not increase by extending the photoperiod from 16/8 h to continuous illumination seems to contradict previous results obtained in photo sequencing batch reactors.[27,47] Probably, this behavior can be attributed to an interplay between light penetration and biomass concentration, which may have a relevant role in MPBRs at long SRTs.[48] Therefore, results suggest that it may be difficult to increase biomass concentration up to 3.0–3.5 g L^{-1} due to self-shading effect, as previously reported in MPBR studies.[49,50]

As the nature of the biomass varies with the microbial community, volatile matter and elemental composition were analyzed at the different photoperiods (Fig. 2b). Volatile fraction increased from 25.9 to 37.3% when extending the lighting period from the control condition (0/24 h) to the 16/8 h photoperiod. Again, no further increment was obtained with the continuous illumination ($p > 0.05$). This volatile content was mainly attributed to microalgae growth, where CO_2 fixation was expected due to photosynthetic activity. Indeed, consistent C/N mass ratios (5.0–5.4) for microalgae biomass[51] were only detected for the MPBR under lighting conditions (Fig. 2c). Nevertheless, it should be noted that no significant variations were observed in the C/N ratios for the

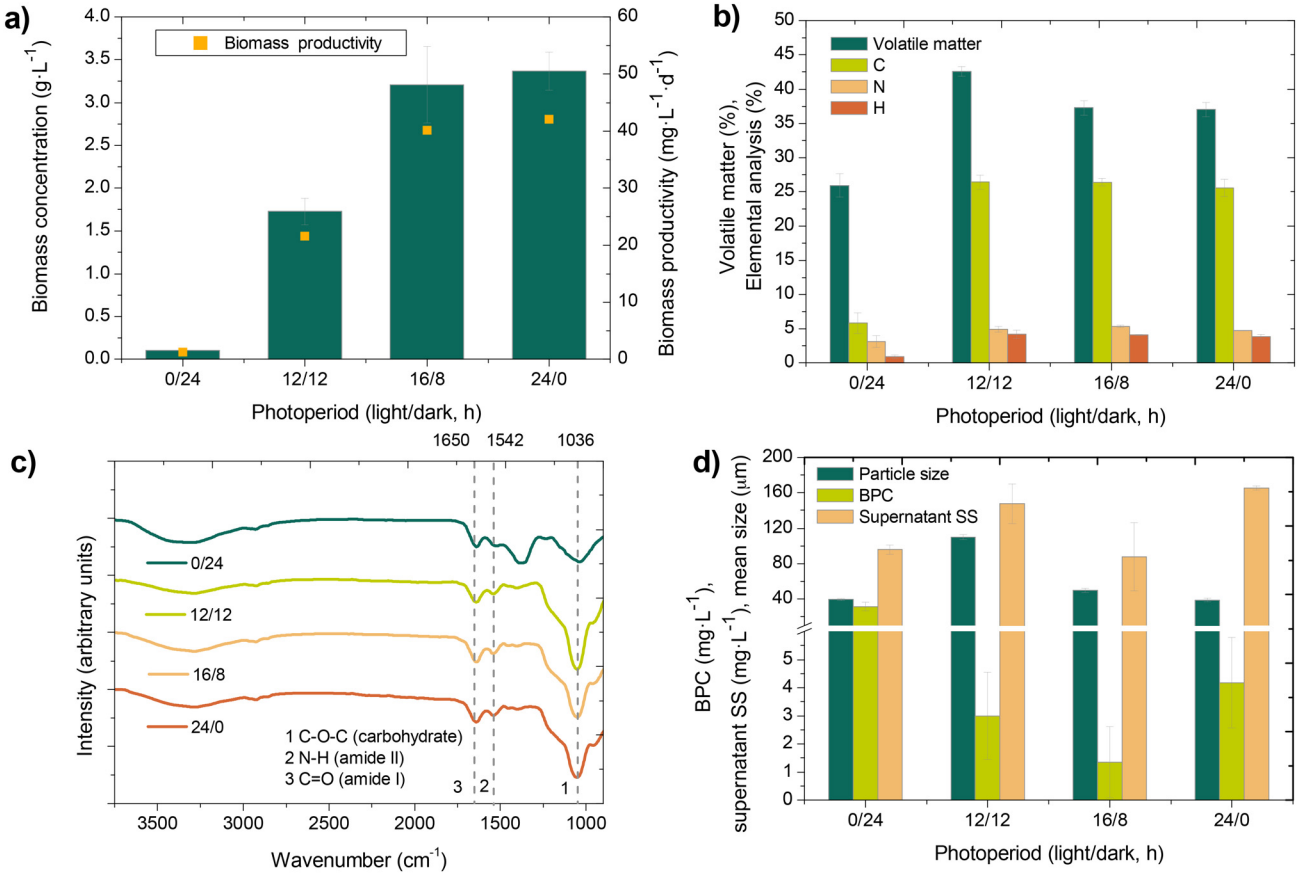

Fig. 2 Effect of the photoperiod on biomass concentration and productivity (n = 15) (a), volatile matter and elemental analysis (n = 3) (b), FTIR spectra (n = 3) (c), and BPC (n = 15), supernatant suspended solids (SS) (n = 3) and mean particle size (n = 3) (d). Elemental analysis data are provided as % wt and dry basis.

different photoperiods, so this parameter could not be related to the ratio of microalgae to bacteria in the biomass. In contrast, the low ratio at 0/24 h can be attributed to low organic carbon in the feedwater (Table 1). Moreover, the ratios of the intensity of the peak assigned to carbohydrate (C–O–C) bonds to the intensity of the specific peaks assigned to proteins (N–H and C═O) in the Fourier transform infrared (FTIR) spectra were probably a result of a higher carbohydrate-to-protein ratio for the MPBR at lighting conditions (Fig. 2c), consistent with the result of the elemental analysis. As reported in the literature, carbohydrates and proteins are major components of the bound extracellular polymeric substances (EPS), which are key in bioflocculation.[8] Since carbohydrate facilitate cell adhesion,[52] a consistent carbohydrate-to-protein ratio can be related to efficient flocculation. This is in accordance with the higher mean particle size obtained in the MPBR under lighting conditions (Fig. 2d). Apparently, microalgal-bacterial consortia enhanced the formation of larger flocs, which agrees with previous studies.[36] However, mean floc size decreased from 104.9 to 38.9 μm while extending the lighting period from 12/12 h to continuous illumination. Particle size distribution has been attributed to microalgae/bacteria proportion, where partial inhibition of microalgae growth results in larger flocs.[31] In this study, results showed smaller flocs at continuous illumination, which can be justified by the increased microalgae growth (reflected by the higher biomass concentration) associated with the extension of the lighting period.

Due to the biological activity in the MPBR, hydrolysis of EPS and decay products generate soluble microbial products (SMP) and biopolymer clusters (BPC).[53] Due to their larger size, BPC were retained by the membrane and can lead to severe membrane fouling.[38] It was observed that the photoperiod had a significant impact on BPC content (Fig. 2d). Under the control condition, BPC accumulated the most significantly (31.1 ± 6.6 mg L^{-1}), which can be related to the low biomass concentration due to carbon-limited conditions imposed (*i.e.* low influent COD and long HRT). A previous study has demonstrated that endogenous conditions may induce cells lysis and biopolymer release in a MBR fed with a secondary effluent.[54] By contrast, very low BPC contents were found in the MPBR, which achieved a minimum at 16/8 h photoperiod ($p < 0.05$). This is probably due to favorable growth conditions for the microalgal-bacterial consortia, where cells lysis and biopolymers release were minimized. In addition, due to a probable higher abundance of heterotrophic bacteria (see section 3.2),

biopolymers are expected to be degraded into smaller compounds.[38] A similar trend was also observed for supernatant suspended solids, which decreased at the 16/8 h photoperiod ($p < 0.05$).

3.2. Treatment performance

In order to assess treatment performance, feedwater and permeate concentration of dissolved organic carbon (DOC), nitrogen–ammonium ($N\text{–}NH_4^+$), total dissolved inorganic nitrogen (DIN) and phosphorus–phosphate ($P\text{–}PO_4^{3-}$) were analyzed. Inherent parameter fluctuation in feedwater can be observed, which was particularly evident in the low nitrogen content at 12/12 h photoperiod run (Fig. 3b). As showed in Fig. 3a, DOC removal was significantly increased (approximately 9-fold increase) in the MPBR under lighting conditions, suggesting significant activity of heterotrophic bacteria in the mixed consortia. As stated, this affects process performance positively by decreasing BPC content. In addition, significant DOC permeate concentration has a negative effect on subsequent processes, such as disinfection byproducts.[55]

The ammonium in feedwater varied between 23.0 and 6.3 mg L^{-1} for the different conditions (Fig. 3b). A complete nitrification was achieved in all cases, obtaining a nitrogen–ammonium content in the permeate below 0.7 mg L^{-1}, where DIN in the permeate was mainly in form of nitrate (>96%), revealing the presence of nitrifying bacteria. In addition, DIN removal significantly increased from 3.5% to 18.1% with increasing photoperiods from control condition (0/24 h) to 16/8 h ($p < 0.05$) (Fig. 3c). However, no further improvement was observed at continuous illumination ($p > 0.05$). At 16/8 h, the average removal rate was 4.71 mg N L^{-1} d^{-1}, consistent with previous studies with similar biomass productivities.[56,57] Since pH was always maintained at similar values (8.1–8.9) under all conditions, the observed increment of nutrient removal was mainly associated with biomass assimilation. As recently reviewed,[58] feedwater ammonium leads to microalgae-nitrifying bacteria competition, which negatively affects nitrogen removal rate. To overcome this issue, operation at short to moderate SRTs has been proposed.[16,37] Nevertheless, a lower SRT would lead to significantly lower biomass concentration and thus increase harvest costs.[8] In addition, long SRTs can decrease BPC and therefore, minimize membrane fouling.[42]

The phosphate concentration in the feedwater and the permeate are showed in Fig. 3d. A similar trend as that

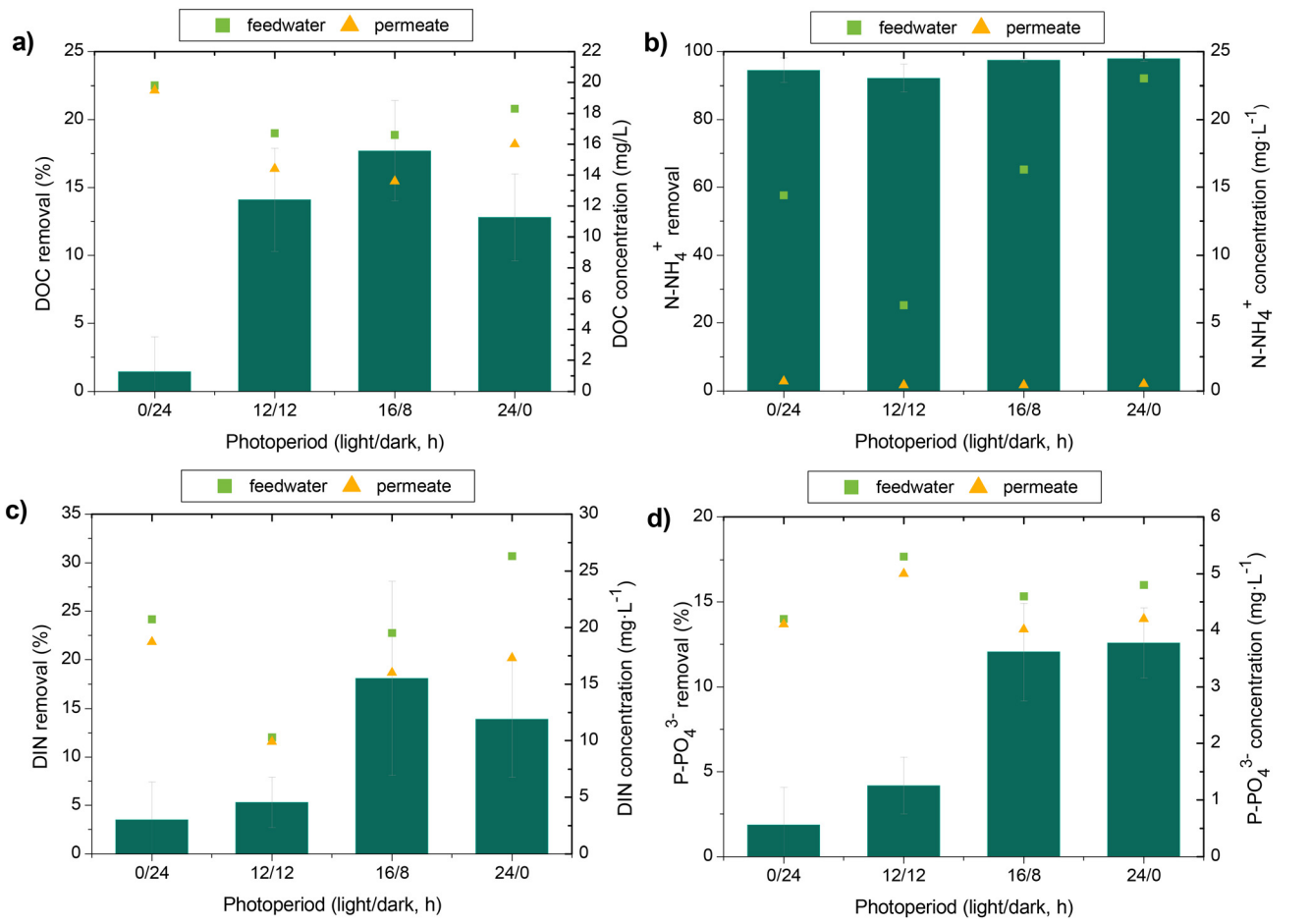

Fig. 3 Influence of the photoperiod on the removal of DOC (a), $N\text{–}NH_4^+$ (b), DIN (c) and $P\text{–}PO_4^{3-}$ (d). Error bars represent the standard deviation (n = 15).

observed for nitrogen removal was found, where photoperiod increased the phosphate removal. A maximum value of 12.1% was obtained for 16/8 h photoperiod, which did not significantly increase at continuous illumination ($p > 0.05$). This can be attributed to a higher biomass productivity when compared with the control condition or the 12/12 h photoperiod. The calculated phosphate removal rate was 0.67 mg L^{-1} d^{-1}, comparable with those reported in previous studies.[48,57]

Finally, it is important to note that the membrane provided a high quality effluent in terms of microbial (absence of *E. coli* and *Legionella* spp.) and physical (turbidity <0.5 NTU) parameters, which complied with the new European regulation of minimum requirements for the use of reclaimed water quality for agricultural irrigation.[59]

In summary, results demonstrate consistent organic matter and nutrient removal rates in MPBR under lighting conditions. Removal rates were influenced by the photoperiod, where maximum values were obtained at 16/8 h, mainly due to greater biomass productivity. No further improvement was attained at continuous illumination, probably due to self-shading caused by the high biomass concentration at long SRTs. Therefore, future work should focus on improving MPBR design to optimize light utilization by reducing culture depth and allow biomass productivities and nutrient removal rates comparable to those obtained at short SRTs.

3.3. Membrane fouling

3.3.1. Reversible fouling characterization: flux step experiments. The effect of the photoperiod on fouling propensity was investigated by conducting the flux-step method,[43] using the reversible fouling rate (r_f = dTMP/dt) as the fouling parameter (Fig. 4). It should be noted that applying lab-scale results to full-scale plant operation may be limited due to certain differences in hydrodynamics.[60] Nevertheless, despite these limitations, lab-scale experiments are useful for elucidating fouling propensity for the different conditions tested, mainly based on the effect of different light/dark photoperiods on biomass properties and biopolymer accumulation. Given the importance of dispersed cells and BPC in the fouling process,[61] the results were compared, under the same experimental conditions, with those obtained while filtering the non-settleable fraction of the suspension. It should be noted that there was no appreciable sedimentation in the control suspension, therefore fractionation could not be carried out. In all cases, an exponential relationship was observed, in accordance with most studies of fouling rate trends in MBRs.[62,63] Therefore, a

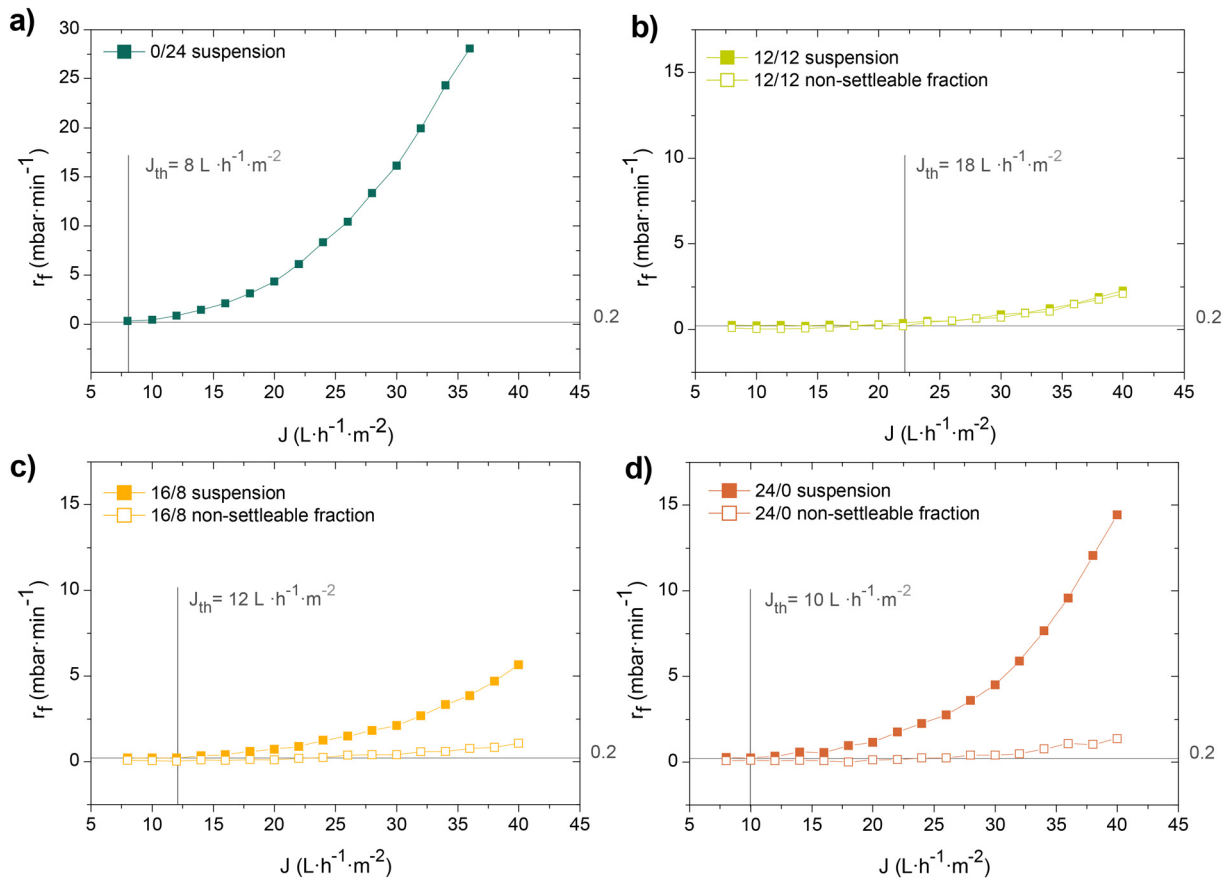

Fig. 4 Fouling characterization by flux stepping experiments. Reversible fouling rate (r_f) of the suspension and non-settleable fraction against permeate flux (J) for the different photoperiods: a) 0/24 h; b) 12/12 h; c) 16/8 h and d) 24/0 h. Threshold fluxes (J_{th}) are determined at each condition.

threshold flux (J_{th}) that separates low and high fouling regions can be identified.[64] A reference value for the fouling rate of 0.2 mbar min^{-1} was assumed which is within the typical range (0.1–1 mbar min^{-1}) reported for reversible fouling rates occurring in full-scale MBRs.[33] Results did not show a linear correlation between the photoperiod and J_{th}, which varied within the range of 8–18 L h^{-1} m^{-2}. Such variation can be explained by the different suspension characteristics. Many previous studies have emphasized the importance of biomass concentration, supernatant biopolymers content and floc size distribution on fouling propensity in MPBRs.[30,35–37,65] Consistently, the lower J_{th} obtained for the control condition (0/24 h) may be attributed to significant BPC accumulation (Fig. 2d). Under lighting conditions, due to lower BPC content, the non-settleable fraction showed a low fouling propensity in all cases (Fig. 4b–d). Therefore, differences in J_{th} may be related to the variations in settleable solid concentration and size. In the case of the suspension at 12/12 h photoperiod, due to its lower biomass concentration, the contribution of settleable solids was negligible and the r_f curve was similar to that obtained for the non-settleable fraction (Fig. 4b). Consequently, the highest J_{th} was attained. This can be explained by the effect of shear conditions associated with air scouring in preventing solids deposition onto the membrane.[66] However, this efficiency declines with increasing solids concentration, resulting in cake layer development.[63] This may explain the relevant contribution of settleable solids at fluxes above the J_{th} and photoperiods of 16/8 and 24/0 h. The increasing trend of fouling rates with the permeate flux also supports the cake development mechanism.[67] Therefore, due to the similar biomass concentrations of the 16/8 and 24/0 h photoperiods, lower fouling rates at the former were consistent with the higher mean floc size. In accordance with previous studies,[31,39] these results suggest that although there is a positive effect of microalgae growth in the mixed culture bioflocculation (BPC decrease and floc size increase), an excessive microalgae/bacteria proportion led to a floc size decrease and higher fouling propensity.

3.3.2. Long-term fouling evolution. To assess residual fouling evolution, long-term tests were conducted under temporized filtration/backwashing cycles (Fig. 5). As previously reported, the residual fouling was characterized by the transmembrane pressure after each backwashing.[43] A permeate flux of 10 L h^{-1} m^{-2} was selected, which according to previously determined threshold values, appeared reasonable to achieve long-term sustainable conditions.[64] This value was comparable with those typically reported in MPBR studies, generally in the range 1.5–17 L h^{-1} m^{-2}.[31,35,39]

Throughout the assays, TMP_i increases as a consequence of residual fouling, regardless of the low permeate flux

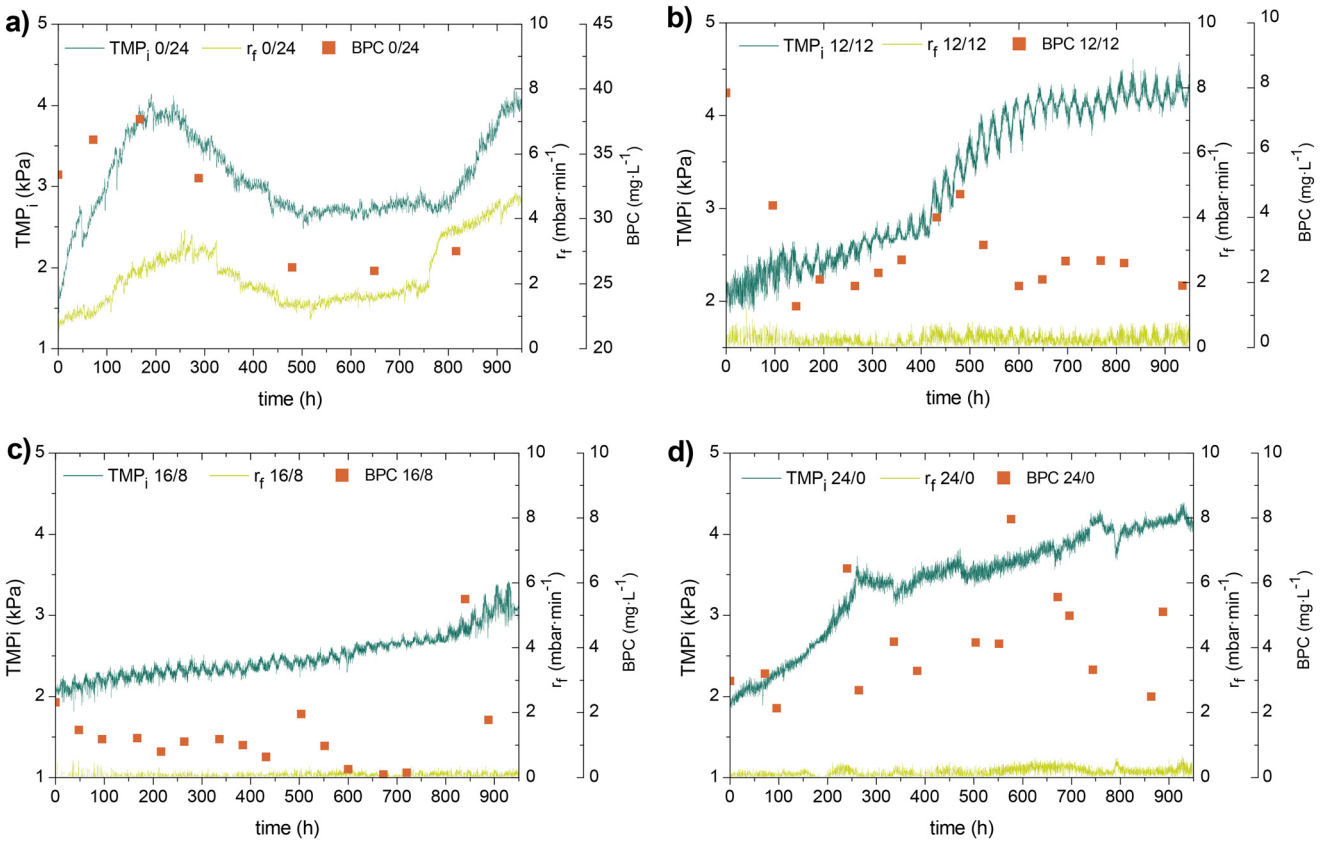

Fig. 5 Fouling evolution during long-term tests. Initial transmembrane pressure (TMP_i), reversible fouling rate (r_f) and BPC for the different photoperiods: a) 0/24 h; b) 12/12 h; c) 16/8 h and d) 24/0 h.

applied (below the threshold one for 12/12, 16/8 and 24/0 h photoperiods). As expected, the high fouling rates obtained for the control condition (0.6–4.8 mbar min^{-1}) led to rapid residual fouling development (Fig. 4a). However, values higher than 4.3 kPa were not reached, observing some fluctuations that seem to correspond to variations in BPC over experimentation time. This reflects an effective control of residual fouling due to the physical cleaning applied. By contrast, under lighting conditions, TMP_i tended to increase continuously at a low rate (0.9×10^{-3}–2.2×10^{-3} kPa h^{-1}, equivalent to 1.5×10^{-4}–3.7×10^{-4} mbar min^{-1}), consistent with the very low fouling rates observed (0.1–0.3 mbar min^{-1}) and BPC content. Optimal performance was achieved at 16/8 h photoperiod, corresponding to the minimal BPC accumulation. Again, results suggest that excessive light irradiation may negatively affect filtration performance.

In addition, membrane recovery by physical and cleaning methods was analysed. Most residual fouling was removed by physical means (rinsing with tap water), revealing external biocake development (Fig. 6a). This was supported by images of the membrane (Fig. 6b–e), in which significant differences in biocake morphology were observed. A dense and compact layer was found for the control condition (Fig. 6b) in contrast to the porous and heterogeneous biocake formed under lighting conditions (Fig. 6c–e). As reported in previous studies, slight biocake formation is inevitable regardless of the physical cleaning (*i.e.* air scouring and backwashing) applied.[31,32] Nevertheless, the results obtained in this study showed a less attached and non-homogeneous biocake layer for the MPBR under lighting conditions, probably due to low BPC accumulation in the supernatant at the tested conditions. Generally, it is reported that biofouling development begins after the formation of an organic conditioning layer on the support.[68] This is corroborated by the hydraulic resistances obtained after rising, which declined when cleaning with an oxidant (Fig. 6a). Also, this organic film was clearly observed in membrane images (-Fig. 6f–i), which disappeared after cleaning (Fig. 6j–m). In addition, some level of inorganic fouling was obtained, but the membrane was completely recovered by the acid cleaning (Fig. 6a).

4. Conclusions

This study has demonstrated the significant effect of photoperiod on the performance of a microalgal-bacterial membrane photobioreactor (MPBR) treating real secondary wastewater effluent. Under the long SRT applied (80 d), biomass productivity and nutrient removal increased with the length of the light period up to a saturation point at 16/8 h (light/dark), above which the effect became insignificant. Subsequently, increasing illumination above saturation deteriorated bioflocculation, decreasing particle size and increasing biopolymer cluster content. This negatively impacted membrane performance by decreasing the sustainable (*i.e.*, threshold) permeate flux and enhancing biocake layer growth during long-term operation.

Development of MPBR technology requires appropriate values of operating parameters, which can maximize biomass productivity and nutrient removal without worsening membrane performance. This work has revealed that the photoperiod is a crucial parameter to be considered.

Author contributions

Segredo-Morales, E.: investigation, data curation, writing – original draft. González, E.: conceptualization, methodology, visualization, funding acquisition, project administration,

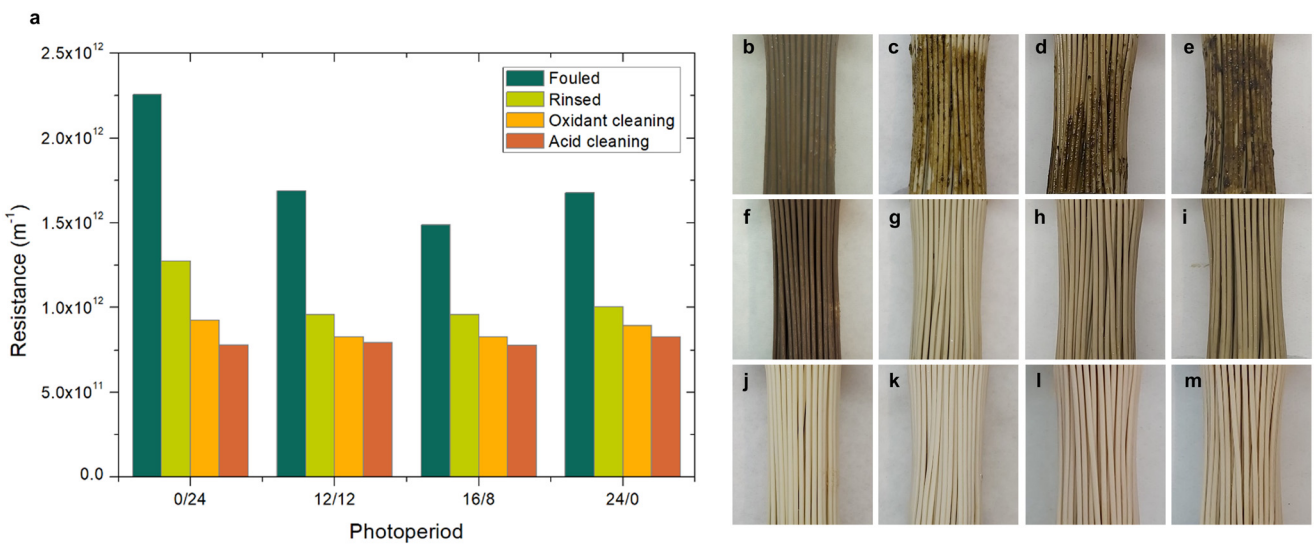

Fig. 6 (a) Recovery of long-term fouled membranes after cleaning protocol: hydraulic resistances of fouled, rinsed and chemical cleaned (oxidant and acid) membranes for the different photoperiods. Images of the fouled membranes for 0/24 h (b), 12/12 h (c), 16/8 h (d) and 24/0 h (e); after rising for 0/24 h (f), 12/12 (g), 16/8 h (h) and 24/0 h (i); and after cleaning with an oxidant for 0/24 h (j), 12/12 h (k), 16/8 h (l) and 24/0 h (m).

writing-review & editing. González-Martín, C.: data curation, writing-review & editing. Vera, L.: conceptualization, methodology, funding acquisition, project administration, supervision, writing-review & editing.

Conflicts of interest

There are no conflicts to declare.

Acknowledgements

This work has been funded by the Ministry of Economy and Competitiveness of the Government of Spain, National Agency for Research (AEI) and European Regional Development Fund (ERDF) (Project: RTI2018-093736-B-I00) and by the agreement between the University of La Laguna and the Ministry of Science, Innovation and Universities for RDI actions in the field of smart specialization in the Canary Islands 2018 (ref. 1205_2020). The authors wish to express their gratitude to the Balsas de Tenerife company (BALTEN) for its collaboration, as well as the Research Group Lab "Water Treatment and Reuse"-ULL for analytical advice and to the Research Support General Service (SEGAI) of ULL for analytical support.

References

1 Z. J. Ren and K. Pagilla, *Pathway to water sector decarbonization, carbon capture and utilization*, IWA Publishing, London, UK, 2022.
2 A. Soares, *Environ. Sci. Ecotechnology*, 2020, **2**, 100030.
3 N. Liu, Y. Dang, B. Hu, M. Tian, H. Jiang, G. Quan, R. Qiao, J. Lei and X. Zhang, *Surf. Interfaces*, 2022, **35**, 102472.
4 H. Li, J. Yu, Y. Gong, N. Lin, Q. Yang, X. Zhang and Y. Wang, *Sep. Purif. Technol.*, 2023, **307**, 122716.
5 J. Yu, H. Li, N. Lin, Y. Gong, H. Jiang, J. Chen, Y. Wang and X. Zhang, *Catalysts*, 2023, **13**, 148.
6 Y. Wang, Y. Gong, N. Lin, L. Yu, B. Du and X. Zhang, *J. Colloid Interface Sci.*, 2022, **606**, 941–952.
7 J. J. J. Y. Yong, K. W. Chew, K. S. Khoo, P. L. Show and J. S. Chang, *Biotechnol. Adv.*, 2021, **47**, 107684.
8 A. Fallahi, F. Rezvani, H. Asgharnejad, E. Khorshidi, N. Hajinajaf and B. Higgins, *Chemosphere*, 2021, **272**, 129878.
9 R. Mu, Y. Jia, G. Ma, L. Liu, K. Hao, F. Qi and Y. Shao, *Water Environ. Res.*, 2021, **93**, 1217–1230.
10 A. Morillas-España, T. Lafarga, A. Sánchez-Zurano, F. G. Acién-Fernández and C. González-López, *Chemosphere*, 2022, **291**, 132968.
11 C. Zhang, S. Li and S. H. Ho, *Bioresour. Technol.*, 2021, **342**, 126056.
12 G. Mannina, H. Gulhan and B. J. Ni, *Bioresour. Technol.*, 2022, **363**, 127951.
13 J. R. Werber, C. O. Osuji and M. Elimelech, *Nat. Rev. Mater.*, 2016, **1**, 16018.
14 P. Kehrein, M. Jafari, M. Slagt, E. Cornelissen, P. Osseweijer, J. Posada and M. van Loosdrecht, *Water Reuse*, 2021, **11**, 705–725.
15 M. Zhang, L. Yao, E. Maleki, B. Q. Liao and H. Lin, *Algal Res.*, 2019, **44**, 101686.
16 J. González-Camejo, P. Montero, S. Aparicio, M. V. Ruano, L. Borrás, A. Seco and R. Barat, *Water Res.*, 2020, **172**, 115499.
17 M. Zhang, K. T. Leung, H. Lin and B. Liao, *Chemosphere*, 2020, **261**, 128199.
18 A. F. Novoa, L. Fortunato, Z. U. Rehman and T. O. Leiknes, *Bioresour. Technol.*, 2020, **309**, 123348.
19 E. González, O. Díaz, I. Ruigómez, C. R. de Vera, L. E. Rodríguez-Gómez, J. Rodríguez-Sevilla and L. Vera, *Bioresour. Technol.*, 2017, **239**, 528–532.
20 Y. Liao, A. Bokhary, E. Maleki and B. Liao, *Bioresour. Technol.*, 2018, **264**, 343–358.
21 K. Li, Q. Liu, F. Fang, R. Luo, Q. Lu, W. Zhou, S. Huo, P. Cheng, J. Liu, M. Addy, P. Chen, D. Chen and R. Ruan, *Bioresour. Technol.*, 2019, **291**, 121934.
22 Y. Luo, P. Le-Clech and R. K. Henderson, *Water Res.*, 2018, **138**, 169–180.
23 M. Wang, R. Keeley, N. Zalivina, T. Halfhide, K. Scott, Q. Zhang, P. van der Steen and S. J. Ergas, *J. Environ. Manage.*, 2018, **217**, 845–857.
24 M. Raeisossadati, N. R. Moheimani and D. Parlevliet, *Renewable Sustainable Energy Rev.*, 2019, **101**, 47–59.
25 C. Vergara, R. Muñoz, J. L. Campos, M. Seeger and D. Jeison, *Int. Biodeterior. Biodegrad.*, 2016, **114**, 116–121.
26 M. M. Maroneze, S. F. Siqueira, R. G. Vendruscolo, R. Wagner, C. R. de Menezes, L. Q. Zepka and E. Jacob-Lopes, *Bioresour. Technol.*, 2016, **219**, 493–499.
27 H. Jia and Q. Yuan, *J. Water Process. Eng.*, 2018, **26**, 108–115.
28 J. González-Camejo, A. Viruela, M. V. Ruano, R. Barat, A. Seco and J. Ferrer, *Algal Res.*, 2019, **40**, 101511.
29 M. Atta, A. Idris, A. Bukhari and S. Wahidin, *Bioresour. Technol.*, 2013, **148**, 373–378.
30 J. González-Camejo, A. Jiménez-Benítez, M. V. Ruano, A. Robles, R. Barat and J. Ferrer, *J. Environ. Manage.*, 2019, **245**, 76–85.
31 M. Zhang, K. T. Leung, H. Lin and B. Liao, *Chemosphere*, 2021, **282**, 131015.
32 L. Fortunato, A. F. Lamprea and T. O. Leiknes, *Sci. Total Environ.*, 2020, **708**, 134548.
33 A. Drews, *J. Membr. Sci.*, 2010, **363**, 1–28.
34 A. L. K. Sheng, M. R. Bilad, N. B. Osman and N. Arahman, *J. Cleaner Prod.*, 2017, **168**, 708–715.
35 S. L. Low, S. L. Ong and H. Y. Ng, *Chem. Eng. J.*, 2016, **290**, 91–102.
36 M. Zhang, K. T. Leung, H. Lin and B. Liao, *J. Environ. Chem. Eng.*, 2021, **9**, 105500.
37 Y. Luo, P. Le-Clech and R. K. Henderson, *Algal Res.*, 2020, **50**, 102013.
38 Y. Luo, R. K. Henderson and P. Le-Clech, *Algal Res.*, 2019, **44**, 101682.
39 L. Sun, Y. Tian, J. Zhang, H. Li, C. Tang and J. Li, *Chem. Eng. J.*, 2018, **343**, 455–459.
40 J. González-Camejo, S. Aparicio, A. Jiménez-Benítez, M. Pachés, M. V. Ruano, L. Borrás, R. Barat and A. Seco, *Water Res.*, 2020, **172**, 115518.

41 Y. Luo, P. Le-Clech and R. K. Henderson, *Algal Res.*, 2017, **24**, 425–437.
42 E. Segredo-Morales, E. González, C. González-Martín and L. Vera, *J. Water Process. Eng.*, 2022, **49**, 103200.
43 E. González, O. Díaz, E. Segredo-Morales, L. E. Rodríguez-Gómez and L. Vera, *Ind. Eng. Chem. Res.*, 2019, **58**, 1373–1381.
44 L. Vera, E. González, O. Díaz, R. Sánchez, R. Bohorque and J. Rodríguez-Sevilla, *J. Membr. Sci.*, 2015, **493**, 8–18.
45 APHA, *Standard Methods for the Examination of Water and Wastewater*, Washington, DC, USA, 21st edn, 2005.
46 S. G. Berk and J. H. Gunderson, *Wastewater Organisms A Color Atlas*, CRC Press, Florida, USA, 1st edn, 1993.
47 C. S. Lee, H. S. Oh, H. M. Oh, H. S. Kim and C. Y. Ahn, *Bioresour. Technol.*, 2016, **200**, 867–875.
48 A. Solmaz and M. Işik, *BioEnergy Res.*, 2019, **12**, 197–204.
49 S. K. Parakh, P. Praveen, K. C. Loh and Y. W. Tong, *Bioresour. Technol.*, 2020, **315**, 123822.
50 P. Praveen, W. Xiao, B. Lamba and K. C. Loh, *Algal Res.*, 2019, **40**, 101487.
51 P. E. A. Debiagi, M. Trinchera, A. Frassoldati, T. Faravelli, R. Vinu and E. Ranzi, *J. Anal. Appl. Pyrolysis*, 2017, **128**, 423–436.
52 O. Orgad, Y. Oren, S. L. Walker and M. Herzberg, *Biofouling*, 2011, **27**, 787–798.
53 Y. Shi, J. Huang, G. Zeng, Y. Gu, Y. Hu, B. Tang, J. Zhou, Y. Yang and L. Shi, *Rev. Environ. Sci. Biotechnol.*, 2018, **17**, 71–85.
54 O. Díaz, L. Vera, E. González, E. García and J. Rodríguez-Sevilla, *Environ. Sci. Pollut. Res.*, 2016, **23**, 8951–8962.
55 H. Y. He, W. Qiu, Y. L. Liu, H. R. Yu, L. Wang and J. Ma, *Water Res.*, 2021, **190**, 116690.
56 A. Solmaz and M. Işık, *Sustain. Energy Technol. Assess.*, 2019, **34**, 1–8.
57 A. Solmaz and M. Işık, *Biomass Bioenergy*, 2020, **142**, 105809.
58 J. González-Camejo, S. Aparicio, M. Pachés, L. Borrás and A. Seco, *Algal Res.*, 2022, **61**, 102563.
59 European Parliament and the Council 2020/741, *Off. J. Eur. Union*, 2020, **177**(33), 32–55.
60 M. Kraume, D. Wedi, J. Schaller, V. Iversen and A. Drews, *Desalination*, 2009, **236**, 94–103.
61 Y. Zhang and Q. Fu, *Sep. Purif. Technol.*, 2018, **203**, 193–208.
62 P. Buzatu, H. Qiblawey, A. Odai, J. Jamaleddin, M. Nasser and S. J. Judd, *Water Res.*, 2018, **144**, 46–54.
63 A. Robles, M. V. Ruano, J. Ribes, A. Seco and J. Ferrer, *J. Membr. Sci.*, 2013, **444**, 139–147.
64 R. W. Field and G. K. Pearce, *Adv. Colloid Interface Sci.*, 2011, **164**, 38–44.
65 L. Sun, Y. Tian, J. Zhang, L. Li, J. Zhang and J. Li, *Bioresour. Technol.*, 2018, **251**, 311–319.
66 M. Bagheri and S. A. Mirbagheri, *Bioresour. Technol.*, 2018, **258**, 318–334.
67 Y. Jang, H. S. Kim, J. H. Lee, S. Y. Ham, J. H. Park and H. D. Park, *Chemosphere*, 2021, **280**, 130763.
68 C. Thobie, W. Blel, C. Dupré, H. Marec, J. Pruvost and C. Gentric, *Chem. Eng. Process.*, 2022, **175**, 108899.